ELSEVIER

Journal of Nuclear Materials 258–263 (1998) 1657–1663

journal of nuclear materials

Shear punch testing of ^{59}Ni isotopically-doped model austenitic alloys after irradiation in FFTF at different He/dpa ratios

G.L. Hankin [a,*], M.B. Toloczko [b], M.L. Hamilton [c], F.A. Garner [c], R.G. Faulkner [a]

[a] *IPTME, Loughborough University, Leicestershire, LE11 3UT, UK*
[b] *Washington State University, Pullman, WA, USA*
[c] *Pacific Northwest National Laboratory, Richland, WA, USA*

Abstract

In this last of a series of papers describing the evolution of microstructure, void swelling and mechanical properties of model austenitic alloys in response to differences in helium/dpa rates, shear punch testing is used to assess the relative effect of helium generation ratios and various important material and environmental variables. Shear punch data confirm the general trends observed in earlier tensile data derived from the ^{59}Ni isotopic doping experiment. There is a convergence to a common saturation level of yield strength that depends on alloy composition, temperature and displacement rate, but not on starting condition. The approach to saturation can be sensitive to helium/dpa ratio, however, and may depend on the starting state. For reasons not yet known, shear punch tests appear to be more sensitive to such transient differences than are tensile tests.

1. Introduction

The ^{59}Ni isotopic tailoring experiment [1] used an isotopic tailoring approach to evaluate the effect of helium generation rates typical of both fast reactor and fusion reactor environments on the tensile properties of three neutron-irradiated model austenitic alloys: Fe–25Ni–15Cr, Fe–25Ni–15Cr–0.04P and Fe–45Ni–15Cr. Helium generation rates relevant to a fusion reactor were produced by an (n,α) reaction involving ^{59}Ni, an isotope which is not found in natural nickel. Nickel enriched in the ^{59}Ni isotope was extracted from Inconel 600 fracture toughness specimens, which were originally irradiated in the engineering test reactor (ETR). The enriched nickel contained 2% of the ^{59}Ni isotope. The helium to dpa (displacements per atom) ratios obtained were of the order of 0.3–0.5 appm He/dpa for the undoped alloys and 4.4–62 appm He/dpa for the ^{59}Ni-doped alloys. Specimens with low and high helium generation rates were irradiated side by side with active temperature control to ±5°C. In effect, a truly one-variable experiment was devised to study the impact of helium on the evolution of mechanical properties.

Previous papers in this series have addressed the influence of helium on radiation-induced evolution of microstructure and void swelling using microscopy disks, and the evolution of mechanical properties using miniature tensile specimens [2–6]. The applicability of these small tensile specimens to irradiation damage studies was established in a variety of other experiments [7].

The three model alloys were irradiated through as many as four discharges of the fast flux test facility's materials open test assembly (FFTF-MOTA). Each alloy was irradiated both with and without ^{59}Ni content, and was prepared in a 20% cold worked (CW) condition and a solution annealed (SA) condition. The three alloys were prepared in 50-g buttons, which were normalised at 1250°C for 2 h in an argon atmosphere. This was followed by a series of cold rolls and 30-min anneals at 1030°C in argon until the alloys were given a final 20% reduction in thickness to 0.25 mm (0.01 in.). The specimens were then punched from the sheet stock. The solution annealed specimens were heat treated at 1030°C

* Corresponding author. Tel.: +44-1509 223 153; fax: +44-1509 223 949; e-mail: g.l.hankin@lboro.ac.uk.

0022-3115/98/$19.00
PII: S0022-3115(98)00204-9

for 30 min after being deburred and engraved with identifying codes [1]. The tensile results showed in general that all alloys approached saturation levels of strength and ductility that were independent of He/dpa ratio and starting condition, but that were sensitive to the irradiation temperature and dpa rate [2].

Transmission electron microscope (TEM) disks of the three Fe–Ni–Cr alloys were in general irradiated side-by-side with the miniature tensile specimens as part of the ^{59}Ni experiment. These disks were originally intended for microscopy examination and density change measurements. The purpose of the current experiment was to use the TEM disks to also assess the evolution of mechanical properties using another small specimen test technique, namely the shear punch test (SPT). Due to some restrictions on specimen availability, only three of the five original irradiation temperatures could be examined (365°C, 490°C and 495°C). TEM disks were available for both the 20% CW and SA conditions for all three irradiation temperatures. In the previously reported miniature tensile study, only the SA condition was available for the materials irradiated at 495°C. It was therefore not possible to see whether the CW and SA conditions approached the same saturation level at 495°C in the original tensile study.

At 495°C, two different irradiation sequences were available: one three-increment sequence that was completely isothermal, and a second, three-increment sequence in which the first irradiation increment was initially isothermal, then subject to a short over-temperature event, followed by prolonged irradiation at temperatures below 495°C. In the following two increments, the irradiation was again isothermal at 495°C. A comparison of the tensile behaviour of the two different irradiation sequences is shown in Fig. 1 for Fe–15Cr–25Ni and demonstrates that the saturation level is dominated by the final irradiation temperature and is relatively unaffected by previous temperature history. Similar behaviour was observed in the other two alloys.

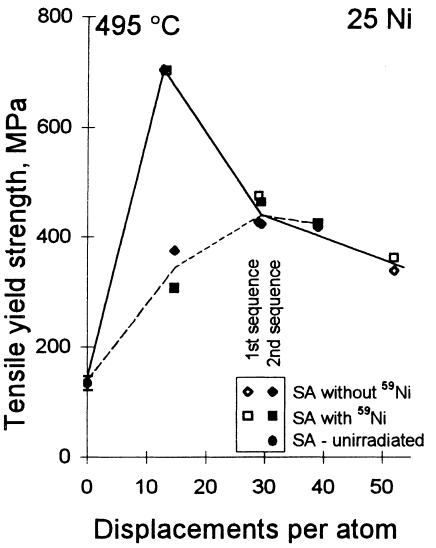

Fig. 1. Convergence of tensile strengths in solution annealed Fe–15Cr–25Ni in two irradiation sequences conducted in FFTF-MOTA [2]. In one sequence (solid line), there was a very irregular temperature history in the first of three irradiation increments, while in the other sequence, all increments proceeded isothermally (dashed line).

2. Experimental

As shown schematically in Fig. 2, the shear punch test is essentially a blanking operation in which a 1 mm diameter punch is driven at a constant rate of 0.127 mm/min (0.005 in./min) through a TEM-sized disk (nominally 0.25 mm thick and 2.8 mm in diameter). The disk is constrained along both its upper and lower surfaces in a fixture, which also guides the punch. The load on the punch is measured as a function of punch travel, which is taken to be equivalent to the crosshead displacement [8].

The curve obtained from a shear punch test is of a similar form to that obtained from a tensile test. Initially a linear relationship exists between load and punch displacement, during which no large scale plastic deformation occurs. This is followed by a deviation from linearity or yield point when permanent penetration of the punch into the specimen occurs. The yield load is taken at the point of deviation from linearity rather than as an offset value as is the case in a tensile test. Beyond the yield point, further deformation forms a shear process zone between the die and punch. Work hardening compensates for reduced 'shear area' until a maximum

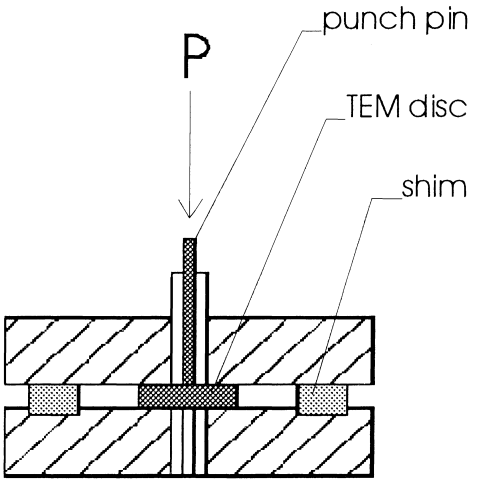

Fig. 2. Cross-section of shear punch test assembly.

load is achieved [8]. Effective shear yield strength (τ_{sy}) and an effective shear maximum strength (τ_{sm}) can be evaluated from the yield and maximum loads, respectively, by the following equation [9]:

$$\tau_{sy,sm} = P_{sy,sm}/(2\pi rt),$$

where $P_{sy,sm}$ is the appropriate load, r is the average of the bore and punch radii and t is the specimen thickness.

3. Results

Two shear punch tests were performed per specimen condition in the case of the irradiated disks and five in the case of the unirradiated controls. The standard deviations in the measured effective shear strength and maximum shear yield strength of the controls were of the order of 15 and 8 MPa, respectively.

Fig. 3 shows both the yield strength data from the shear punch test and the original yield data from the miniature tensile testing for materials irradiated at 365°C. It can be seen for both tensile and shear punch tests that the yield strength measurement of each alloy in both starting conditions saturates before 10 dpa. The yield strength of the 25Ni+P alloy saturates at a slightly higher level than the 25Ni, which in turn saturated with a higher yield strength than the 45Ni alloy. There is no obvious effect of helium level, and the saturation strength is independent of the thermomechanical starting state for the materials irradiated at 365°C. The only significant difference between results of the two types of test is the characteristic lower level of shear yield, compared with that of the tensile yield (see companion paper of Hankin and coworkers, [10]).

The shear punch test results for the alloys irradiated at 490°C at a lower dpa rate (Fig. 4) produce the same general findings as the original tensile results [2]. The yield strength tends to approach a saturation level that is independent of the starting condition. The total exposure at 490°C in this sequence was low (6 dpa) and therefore a common saturation strength for the CW and SA material starting states has not yet been achieved. Once again there was no obvious influence of helium/dpa ratio. The scatter in the data measured from speci-

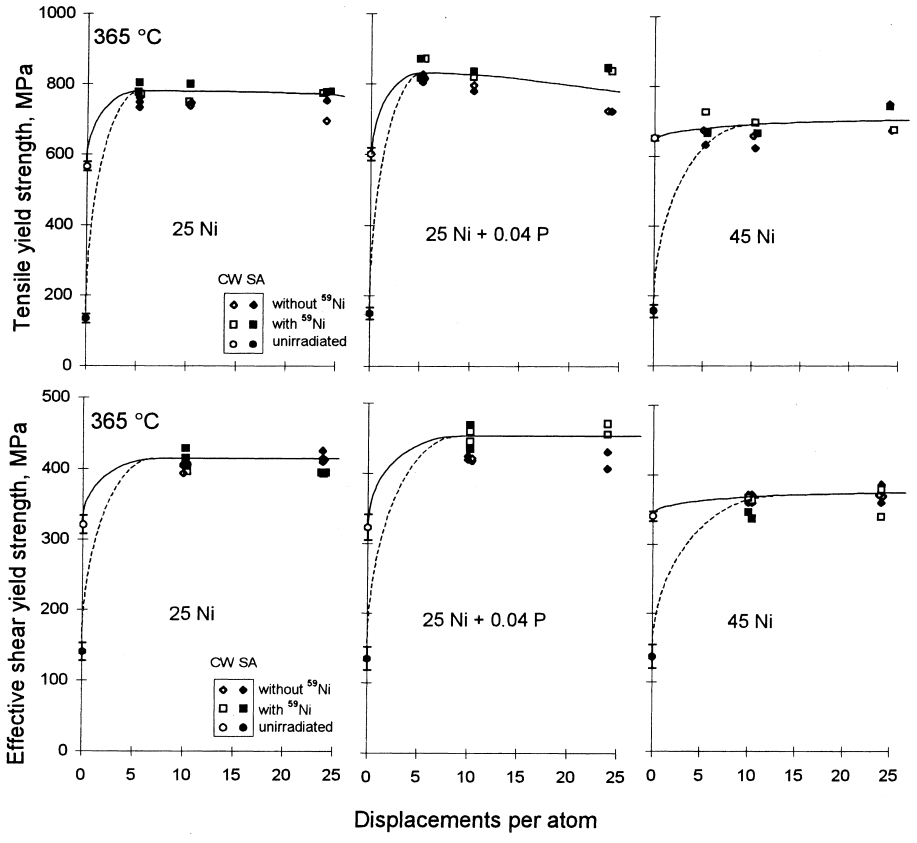

Fig. 3. The influence of thermomechnical starting state and different He/dpa ratios on the tensile yield and shear yield strengths of three austenitic alloys irradiated below the FFTF core at 365°C. He/dpa ratios of 0.5 and 15 appm He/dpa were generated in the undoped and doped alloys, respectively.

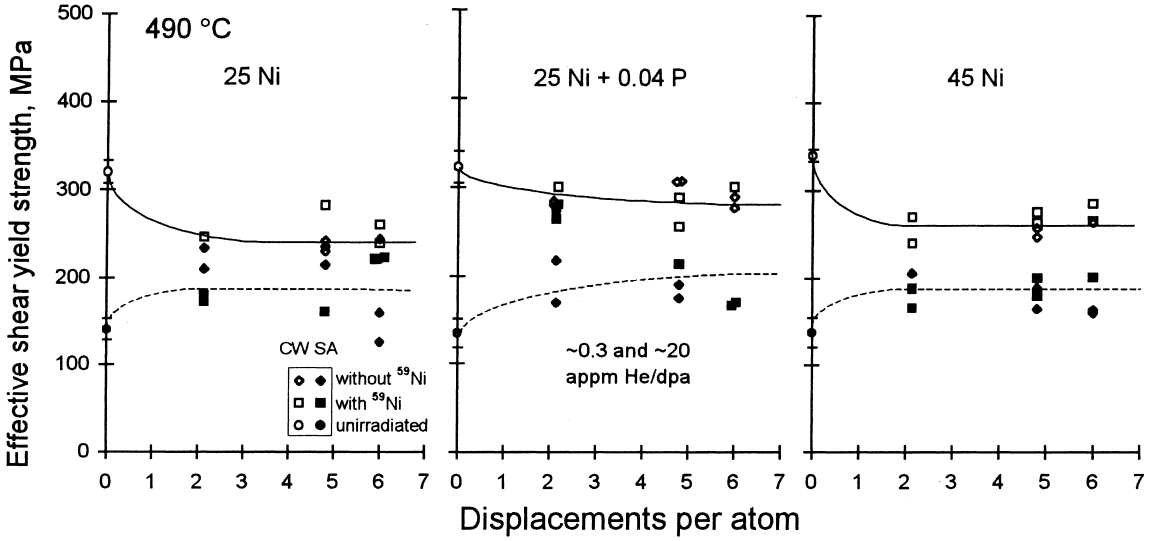

Fig. 4. The influence of thermomechnical starting state and helium generation rates of 0.3 and 20 appm He/dpa on the effective shear yield strength of specimens irradiated at a relatively lower dpa rate above the FFTF core at 490°C (dashed lines indicate SA starting state and solid lines indicate the CW starting state).

mens irradiated at 490°C by the shear punch test was larger than was seen in the miniature tensile data.

The alloys irradiated at 495°C in the fully isothermal sequence, which have accumulated up to 39 dpa at a higher dpa rate, show that they are at a more advanced stage in the saturation of the yield properties than the alloys irradiated at 490°C (Fig. 5). There would appear to be some effect of helium in this series, however, which acts as to strengthen especially the SA Fe–15Cr–45Ni, and to a lesser extent, the 25Ni+P alloy. It is unclear whether there is any significant effect of helium on the shear yield properties in the 25Ni alloy. Most interestingly, the SA and CW specimens in this sequence appear to approach common saturation levels as expected, but levels that are different for the low and high He/dpa specimens. In this case the use of shear punch tests have

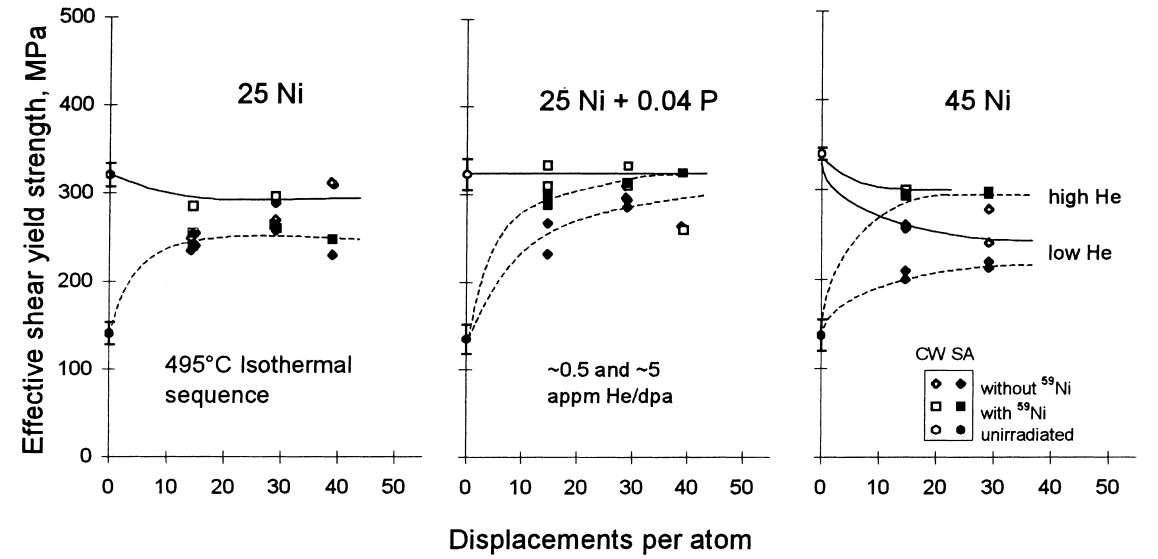

Fig. 5. The influence of starting state and He/dpa ratios of 0.5 and 5 appm He/dpa on the effective shear yield strength of specimens irradiated in the fully isothermal sequence at the bottom of the core of FFTF at 495°C (dashed lines indicate the SA starting state and solid lines indicate the CW starting state).

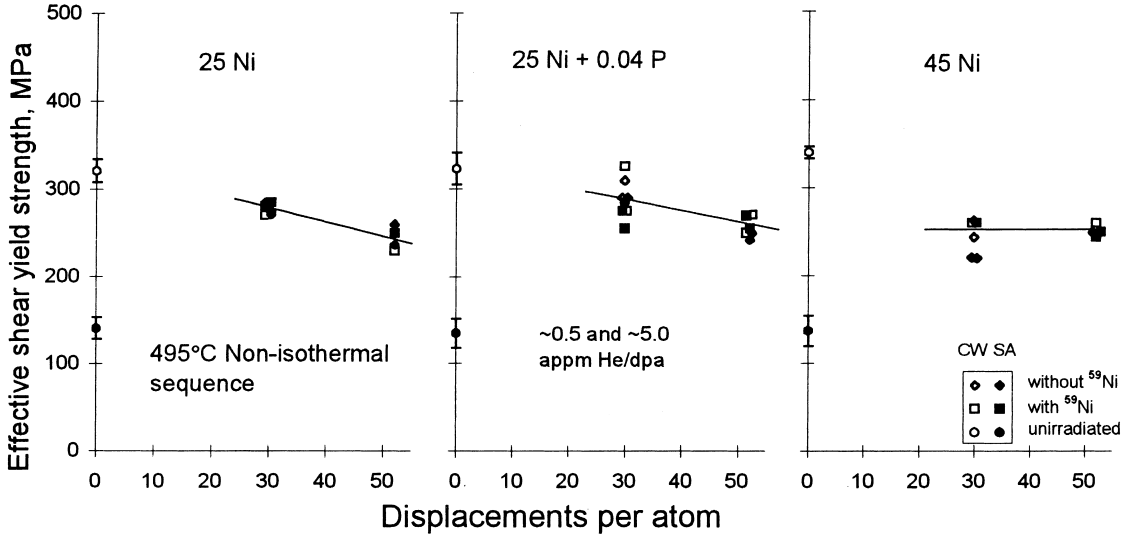

Fig. 6. The influence of starting state and He/dpa ratios on the effective shear yield strength of specimens irradiated in the initially non-isothermal sequence at the bottom of the core of FFTF at 495°.

supplied useful information that would not be obtained from the more limited tensile test matrix, where CW specimens were not available.

The behaviour of specimens irradiated at 495°C, which had experienced the non-isothermal sequence initially, are shown in Fig. 6. In the later stages of the irradiation, the tensile results showed that the yield strength of the materials was still recovering from a peak induced by the lower temperatures in the last portion of the non-isothermal event (Fig. 1). The SPT results shows the same downward trend in yield strength for the two 25Ni alloys. The convergence in yield strength from the SA and CW starting conditions is complete after 52 dpa. The saturation level of the shear yield strength of materials irradiated in the two 495°C sequences is higher than that in the 490°C sequence, reflecting primarily a difference in the displacement rate.

4. Discussion

As might be expected, the shear punch test replicates the trends seen in the original miniature tensile study. This confirms the original findings that the yield strength of each material approached a saturation level that was independent of the thermomechanical starting condition and He/dpa ratio, but sensitive to the irradiation temperature and dpa rate.

The one result which significantly differs from that of the original miniature tensile study is that there appears to be a significant effect of helium on the evolution of the yield properties in the 25Ni+P and especially the 45Ni alloys during the early stages (14–29 dpa) of the isothermal irradiation at 495°C. The tensile test experiment did not include any of the materials in the CW condition and the tensile data for the SA material did not show any obvious difference between the ^{59}Ni doped and the undoped alloys. The shear yield data at 495°C and 29 dpa from the non-isothermal sequence matches that from the fully isothermal sequence at the same dpa level. After 52 dpa, the shear yield strengths of the non-isothermal sequence are showing further convergence at a level that is consistent with that of the isothermal sequence (Fig. 5).

A study of the microstructure of the materials irradiated at 495°C to 14 dpa, which had experienced the non-isothermal event, was reported by Stubbins et al. [4]. The study showed that no precipitates had evolved in any of the alloys at this irradiation temperature and dose, but that the total number of faulted loops and the void density was consistently higher for the ^{59}Ni doped alloys. Kawanishi and coworkers [6] had also commented that the influence of He was to increase network dislocation density of the same materials after irradiation at 365°C and 600°C, but not to such an extent that any large differences in material properties would be evident. The expected result of an increased density of obstacles impeding dislocations in those specimens containing helium would be an increase in the yield strength.

The results of a barrier hardening calculation [10] by the current authors based on microstructural data from the paper of Stubbins et al. [4] are shown in Table 1. In this calculation, the change in yield strength ($\Delta\sigma_y$) from the SA starting state (σ_0) is evaluated as the sum of the total contributions from short and long range obstacle

Table 1
Barrier hardening theory applied to the microstructural data from materials irradiated at 495°C to 14 dpa [4]

Specimen details		Contribution to hardening, $\Delta\sigma_{(obstacle)}$				Total change in yield strength	SA tensile yield strength	Model prediction	Tensile test data
		Cavities	Faulted loops		Network dislocations				
			Large $\phi > 6$ nm	Small $\phi < 6$ nm					
Material	Condition	$\Delta\sigma_c$ (MPa)	$\Delta\sigma_L$ (MPa)	$\Delta\sigma_l$ (MPa)	$\Delta\sigma_n$ (MPa)	$\Delta\sigma_{y(t)}$ [a] (MPa)	σ_0 [b] (MPa)	σ_y [c] (MPa)	σ_y (MPa)
25Ni+P	SA	273	61	43	49	427	150	**577**	738
	SA+He	303	78	76	56	515	150	**665**	789
45Ni	SA	128	47	23	56	253	160	**413**	498
	SA+He	145	82	52	52	330	160	**490**	553
45Ni	CW	72	109	39	63	283	160	443	[d]
	CW+He	85	86	46	63	280	160	440	[d]

[a] Theoretical change in yield strength due to microstructural development during irradiation.
[b] Measured yield strength of unirradiated, solution annealed starting state.
[c] Predicted yield strength after irradiation.
[d] Tensile specimens not available.

types. In this case, the cavities are considered to be short-range, and the faulted loops and network dislocations are treated as long-range. For completeness, it should be mentioned that, had there been more than one type of short-range obstacle, the root mean square value is normally taken as the total short-range contribution. The following general formula was used for each individual obstacle contribution:

$$\Delta\sigma_y = \frac{m\alpha f \mu b}{l},$$

where m is the polycrystalline factor (3.1 for a fcc material), α is a scaling factor for different types of obstacles (for example, $0.8 < \alpha < 1.0$ for cavities and $\sim 0.2 < \alpha < \sim 0.5$ for faulted loops), f is a random array efficiency factor which scales non-linearly with α [11,12], μ is the shear modulus, b is the Burgers vector and l is the inter-obstacle distance on the glide plane based on a square array of obstacles. The value of l was calculated as a function of obstacle density and average obstacle size and the values of ($f\alpha$) used were 0.81 for cavities, 0.33 for both small and large faulted loops and 0.09 for network dislocations. As seen in Table 1, the largest contribution to the value of $\Delta\sigma_y$ for both the SA and SA+He conditions is from the cavities. The large increase in the density of faulted loops in the alloys with a high helium content compared to the alloys with a low helium content was estimated to be of secondary importance in this instance.

The model predictions are consistently lower than the tensile results by ~150 MPa for the 25Ni+P alloy and ~70 MPa for the 45Ni alloy. Assuming a valid model has been selected, this suggests that there might be some component of hardening not accounted for in the model. A similar divergence between model predictions and tensile measurements for Fe–15Cr–*X*Ni (*X* = 25–45) was observed in an earlier experiment on these alloys, and was attributed to radiation-induced spinodal-like decomposition that was absent at 25Ni but increased strongly in the range 35–45Ni [13,14]. Phosphorus is also known to significantly affect dislocation and loop evolution, and to significantly harden the Fe–15Cr–25Ni especially when phosphide precipitates begin to form [15].

A useful result of this exercise is that the tensile data and the model are in agreement on the effect of helium on the yield strength. The model predicts a difference of ~80 MPa between the yield strengths of the high and low helium content alloys in Table 1 and the miniature tensile test results show a corresponding difference of ~50 MPa.

Other papers in the ^{59}Ni series [3,16,17] show that the effect of He on yield strength is usually small when compared with the effects of composition and recent irradiation temperature. However, it would appear from the SPT data that during the early and intermediate stages of irradiation at 495°C, the effect of helium is to accelerate the convergence of the material yield strength towards a saturation level. The material containing lower levels of helium was showing convergence, but at a lower rate. By 52 dpa there is no evidence to show that helium has any effect on the yield properties (Fig. 6).

A comparison of the shear punch test results to those originally obtained by miniature tensile testing indicates that the measured effective shear yield strength is proportional to the tensile yield strengths. The development of an empirical correlation between shear punch and miniature tensile properties is reported elsewhere [10].

5. Conclusions

Shear punch data confirm the general trends observed in earlier tensile data derived from the ^{59}Ni iso-

topic doping experiment. There is a convergence to a common saturation level of yield strength that depends on alloy composition, temperature and displacement rate, but not on starting condition. The approach to saturation can be sensitive to helium/dpa ratio, however, and may depend on the starting state. For reasons not yet known, shear punch tests appear to be more sensitive to such transient differences than are tensile tests.

References

[1] R.L. Simons, H.R. Brager, W.Y. Matsumoto, J. Nucl. Mater. 141–143 (1986) 1057.
[2] F.A. Garner, M.L. Hamilton, L.R. Greenwood, J.F. Stubbins, B.M. Oliver, ASTM-STP 1175 (1993) 921.
[3] J.F. Stubbins, F.A. Garner, J. Nucl. 191–194 (1992) 1300.
[4] J.F. Stubbins, J.E. Nevling, F.A. Garner, R.L. Simons, Fusion Reactor Materials DOE/ER-0313/6 (March 1989) 93.
[5] J.F. Stubbins, F.A. Garner, J. Nucl. Mater. 179–181 (1991) 523.
[6] H. Kawanishi, F.A. Garner, R.L. Simons, J. Nucl. Mater. 179–181 (1991) 511.
[7] F.A. Garner, M.L. Hamilton, H.L. Heinisch, A.S. Kumar, ASTM-STP 1204 (1993) 336.
[8] G.E. Lucas, G.R. Odette, J.W. Sheckherd, ASTM-STP 888 (1986) 112.
[9] M.L. Hamilton, M.B. Toloczko, G.E. Lucas, Recent Progress in Shear Punch Testing, in Miniaturized Specimens for Testing of Irradiated Materials, Hans Ullmaier and Peter Jung, Eds., Forschungszentrum Jülich GmbH (1995) 46.
[10] G.L Hankin, M.B. Toloczko, M.L. Hamilton, R.G. Faulkner, these Proceedings.
[11] M.B. Toloczko, G.E. Lucas, G.R. Odette, R.E. Stoller, M.L. Hamilton, ASTM-STP 1270 (1996) 902.
[12] A.J.E. Foreman, M.J. Makin, Canadian J. Phys. 45 (1967) 511.
[13] H.R. Brager, F.A. Garner, M.L. Hamilton, J. Nucl. Mater. 133134 (1985) 594.
[14] F.A Garner, J.M. McCarthy, Physical Metallurgy of Controlled Expansion Invar-type alloys, Russell, K.C. and Smith, D.F. Eds., The Minerals, Metals and Minerals Society (1990) 18.
[15] M.A. Mitchell, masters thesis, University of Illinois at Urbana-Champaign, 1991.
[16] M.L. Hamilton, F.A. Garner, J. Nucl. Mater. 191–194 (1992) 1239.
[17] F.A. Garner, M.L. Hamilton, R.L. Simons, M.K. Maxon, J. Nucl. Mater. 179–181 (1991) 554.